THE ELABORATION AND CHARACTERIZATION OF A HYBRID BIONIC COATING ON Ti BASED ON HYDROXYAPATITE AND NANOTUBES

Luiza ICHIM[1], Mariana PRODANA[2], Cristina DUMITRIU[3]

The aim of this paper is focused on the elaboration and characterization of a complex hybrid ceramic coating on Ti plates, containing TiO_2 nanotubes obtained by anodizing, single walled carbon nanotubes (SWCNTs) functionalized with –COOH groups and hydroxyapatite. The infrared spectroscopy analysis of the new coating denoting its bionic structure with a bone component as hydroxyapatite and the wettability measurements with contact angle determinations in the hydrophilic domain are strong recommendations for mineralization and osseointegration of such materials able to be used in implants. The electrochemical procedures were conducted in Hank's solution and complete the characterization.

Keywords: TiO_2 nanotubes, single walled carbon nanotubes, hydroxyapatite, open circuit potential

1. Introduction

Despite the fact that titanium and titanium alloys have very good properties as low density and stability, in order to enhance their performance various treatments and modifications including bionic coatings with hydroxyapatite (HA) have been investigated and performed on their surface [1-3]. The coating with hydroxyapatite is a biomimetic one due to the fact that being a bone component its properties from chemical and phase composition point of view, are similar to the bone and tooth mineral components [4,5]. This characteristic feature is very important for bioapplications in obtaining a biocompatible ceramic material based on these properties. Unfortunately there are some drawbacks like its low mechanical strength [6].

The most plausible way to obtain a good material for implants is to combine the chemical and phase properties of HA with the chemical resistance of Ti, an already widely used material for implants [7].

[1]PhD student, Department of General Chemistry, University POLITEHNICA of Bucharest, Romania, e-mail: necula_luiza@yahoo.com
[2]Lecturer, Department of General Chemistry, University POLITEHNICA of Bucharest, Romania, e-mail: prodana_mariana@yahoo.com
[3]Teaching assistant, Department of General Chemistry, University POLITEHNICA of Bucharest, Romania, e-mail: c_dumitriu@chim.upb.ro

We thought that the best way to achieve such material is to alter the surface of the Ti by changing the film (TiO_2) and finding ways to successfully deposit HA on the material [8]. Thus it is obtained a promising way for creating a bioactive implant with better mechanical properties [9]. We remember that the many advantages of Ti and Ti alloys include biocompatibility, good resistance to corrosion, low density and sufficiently strong for use as orthopedic implant materials [10].

For better and safer use, especially in bioapplications, single and multiwall carbon nanotubes require additional treatments as oxidation treatments [11]. Despite their structure, excellent stability and mechanical properties, carbon nanotubes contain many structural defects [12] and have a low chemical reactivity and a low dispersability in polar and non-polar solvents [13]. Due to hydroxyapatite-carbon nanotubes composite coating on Ti plate, an improvement of the properties of HA coatings both from mechanical and biological point of view could be achieved [14]. As regarding biomedical application, the composite (hybrid material) is recommended both, by its bioactivity on the material surface and particular physical properties. Its very good mechanical properties [15] help the achieving the necessary qualities in bone-implant bonding and osseointegration [10].

The present work aims to investigate the preparation and behavior of a new complex hybrid material based on TiO_2 nanotubes, hydroxyapatite, and multiple functionalized carbon nanotubes with carboxyl groups (SWCNT-COOH). Electrochemical stability of the new coating was tested in Hank's solution and established by open-circuit potential (OCP), electrochemical impedance spectroscopy (EIS) and potentiodynamic polarization tests, as well as cyclic voltammetry. Introducing a new coating as TiO_2-HA-SWCNTs, this study aims to present comparatively the behavior in physiological environment of the following materials: TiO_2, TiO_2-HA, TiO_2-HA-SWCNTs.

2. Materials and methods

Single wall carbon nanotubes (SWCNTs) were purchased from Sigma-Aldrich with more than 90% carbon basis and 0.7-1.1 nm diameter. Their oxidation was made using a mixture of 98% sulfuric acid (Merck) and 70% nitric acid (Merck). An Agilent 0.45 μm nylon membrane filter and IsoLab vacuum filtration assembly was used to filter and wash the oxidized SWCNTs.

For structural characterization FT-IR spectra of treated SWCNTs were obtained with a Perkin Elmer Spectrum 100 in the 600-4000 cm^{-1} wavenumber range, 4 cm^{-1} resolution and 32 scans.

SWCNTs purification/oxidation method

Due to the fact that CNTs are difficult to be dispersed in the common solvents and have predisposition to form large aggregates, several approaches were developed to increase their hydrophilic behavior [16]. In this work we proposed an oxidation treatment of SWCNTs using nitric and sulfuric acids at room temperature. This process is also known as carboxylation process [12] and it consists in a covalent attachment of hydrophilic moieties [17].

5 mg of SWCNTs were placed in 10 mL of aqueous H_2SO_4: HNO_3 (2:1) solution under sonication for 8 h at room temperature. By this procedure we obtained SWCNTs functionalized with carboxyl groups. In the second step, the nanotubes were separated by centrifugation, washed with deionized water until the neutral pH (approx. 6.5–7) and filtered through a 0.45 μm membrane filter. Finally, the sample was dried at room temperature.

After drying, the obtained thin, black powder was stored at room temperature in a brown glass vial, until further usage.

Elaboration of complex hybrid coating

The anodization of Ti plates starts with the titanium plates of 1x1 cm^2 which were polished using various emery paper sizes. Afterwards, the samples were rinsed for 15 minutes on ultrasonication bath with distillated water, then with ethylic alcohol and acetone. The anodizing time was 1.5 hours, using 0.5% HF + 5 g/L Na_2HPO_4 solution which is a type I generation of electrolyte [18] used for TiO_2 nanotubes fabrication. After anodizing, the plates were immersed in an aqueous suspension containing 2 g/L SWCNT-COOH, 9.91 g/L $Ca(NO_3)_2x4H_2O$ and 2.875 g/L $NH_4H_2PO_4$ and subjected to a magnetic stirring for 4 hours. In such way the deposition of hybrid material based on SWCNT-COOH and HA is a two steps process involving anodizing and immersion with vigorously stirring.

Coatings characterization

The FT-IR characterization of the SWCNT-COOH coatings has been performed using Perkin Elmer Spectrum 100 FT-IR equipment with a 600÷4000 cm^{-1} domain. The determination of contact angles was performed with CAM 100 apparatus. The procedure supposes to place an equal volume (drop) of distilled water on samples surface. The electrochemical measurements were carried out in 50 mL electrolyte at 37°C using a potentiostat/galvanostat VoltaLab 40 controlled by a computer. The potentials were refered against Ag/AgCl electrode and a platinum electrode was used as an auxiliary electrode.

The electrochemical behavior of these hybrid materials has been investigated by use of open-circuit potential, electrochemical impedance

spectroscopy and potentiodynamic polarization tests and cyclic voltammetry. The evolution in time of the open circuit potential was carried out for 20 minutes, impedance measurements were performed on the frequency range between 100 kHz and 50 mHz with an AC wave of ± 25 mV, the potentiodynamic polarization was carried out between -300 mV and +300 mV with a scan rate of 2 mV/sec and cyclic voltammetry between -800 mV and 1500 mV with a scan rate of 2 mV/sec.

All tests have been performed in Hank's solution, its composition being presented in Table 1.

Table 1

Chemical composition of Hank solution

Electrolyte	Composition
HANK	NaCl-8g/L KCl-0.4g/L $NaHCO_3$-0.35g/L NaH_2PO_4*2H_2O-0.25g/L Na_2HPO_4*2H_2O-0.06g/L $CaCl_2$*2H_2O-0.19g/L $MgCl_2$-0.19g/L MgSO4*7H2O-0.06g/L Glucose-1g/L

3. Results and Discussions

Hybrid materials structure was identified by using infrared spectroscopy (FT-IR). This analysis using transmitter module for coated materials is presented in Fig. 1a and Fig. 1b as spectra for TiO_2-HA and TiO_2-HA-SWCNTs, respetively.

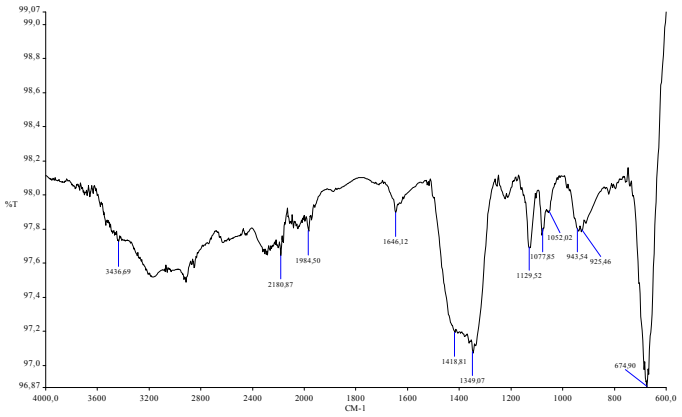

Fig 1a. FT-IR spectra of TiO_2-HA coated material

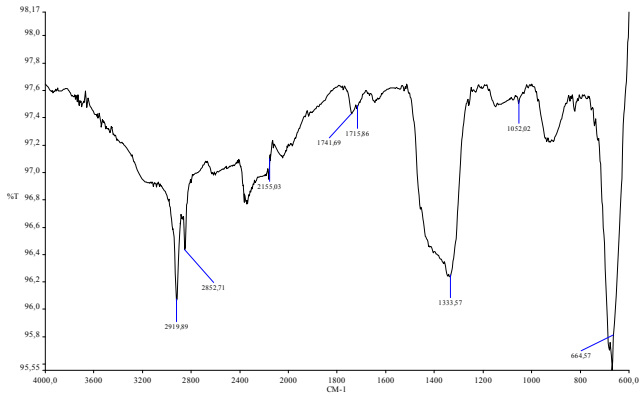

Fig 1b. FTIR spectra of TiO_2-HA –SWCNTs coated material

As expected there are all characteristic for HA bands, according to literature [19]. There are peaks in the 925-943 cm^{-1} range due to asymmetric streching vibrations of P-O-P. At 1001-1077 cm^{-1}, is a main peak together with a less evident one and they are associated to asymmetric streching vibrations of P-O-P bonds. In the 1070-1093 cm^{-1} range there are the streching vibrations of groups PO^{2-} and in 1157-1183 cm^{-1} range there are small peaks due to phosphate terminal groups PO_3^{2-}. The presence of hydroxyl group is indicated around 3400 cm^{-1}. It can be seen that in the constitution of HA coating we observe the presence of the absorption bands by the appearance of two peaks, one at 1333 cm^{-1}, and the second one at 1615 cm^{-1} that can be assigned to carbonate group.

In order to quantify the wettability of a solid surface by a liquid we used the contact angle method. The obtained results for each sample in contact with a distilled water drop are represented in Table 2. All values show a strong hydrophilic character, especially for TiO_2-HA.

Table 2

Values of contact angle for TiO_2, TiO_2-HA, and TiO_2-HA-SWCNTs coatings

Coating	Contact angle, degree	STD %
TiO_2	52.44	0.748
TiO_2-HA	14.45	2.390
TiO_2-HA-SWCNTs	35.95	0.730

The simplest approach of electrochemical behavior of the chosen materials at 37^{o}C is OCP-time curves shown in Fig. 2. From the obtained data in Hank solution it can be seen that the value of OCP remains almost constant in Ti-TiO_2 case, meaning that the material is stable in this electrolyte.

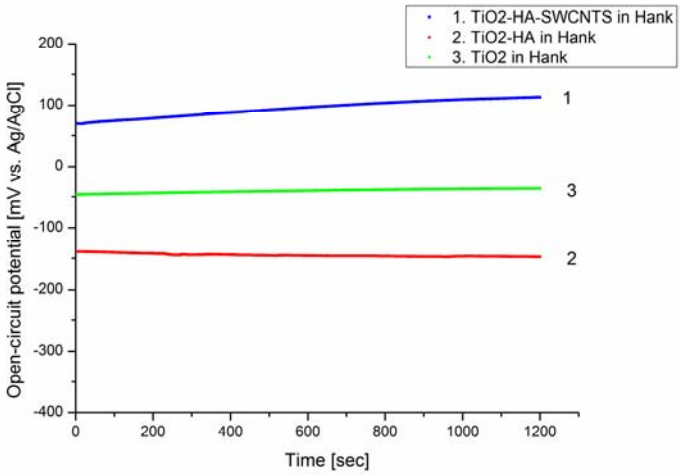

Fig. 2. The OCP versus time for TiO_2, TiO_2-HA,TiO_2-HA-SWCNTs materials in Hank solution at 37°C

The curve for the Ti-TiO_2-HA material, seems to be a little different compared with the other two materials, albeit the values of E_{OCP} initial and E_{OCP} final are very close, the trend is descendant in the beginning period. In the case of Ti-TiO_2-HA-SWCNTs, after 20 minutes, E_{OCP} values remained in slow ascendant trend, which can be explained by the fact that this new hybrid material tends to a nobler state compared with Ti-TiO_2 and Ti-TiO_2-HA. It is to mention as well that all the potential values for this sample in Hank solution are in the positive domain of potential. In Table 3 are represented the variables of the regression equations with the general formula:

$$y = y_0 + A*exp(R_0*x) \quad (1)$$

Table 3

The variables values of the regression equations for E_{OCP}-time dependences

Coating	Electrolyte	y_0	A	R_0	R^2
TiO_2	Hank	-30	-16.562	-0.08340	0.9978
TiO_2-HA	Hank	-147	9.166	-0.00275	0.9757
TiO_2-HA-SWCNTs	Hank	148	-79.122	-0.00072	0.9987

In Table 4 are presented the E_{OCP} values determined for each immersed material for initial time and for 20 minutes immersion in Hank solution. For the studied materials (TiO_2, TiO_2-HA-SWCNTs) we can observe the tendency of the E_{OCP} in time to shift towards more positive values than that determined at the initial moment of immersion, which means that the material presents the tendency

to passivate by forming in time of a passive layer which grows and makes the material more resistant to corrosion processes.

Table 4

E_{OCP} values for each immersed material in Hank solution at 37 °C

Sample	E_{OCP}, mV vs.Ag/AgCl in Hank solution	
	Initial	After 20 min
TiO_2	-47	-36
TiO_2-HA	-139	-148
TiO_2-HA-SWCNTs	70	113

However, for TiO_2-HA material we can observe the tendency of the E_{OCP} in time to evolve to more negative values than that determined at the moment of immersion, this shift towards the active direction being explained probably by a dissolution that occurs at the exposed surface.

For performing potentiodynamic polarization at 37°C, the potential of the working electrode was scanned from 300 mV to -300 mV (vs. Ag/AgCl) with a scan rate of 2 mV/s. The semilogarithmic curves for the three materials are presented in Fig. 3.

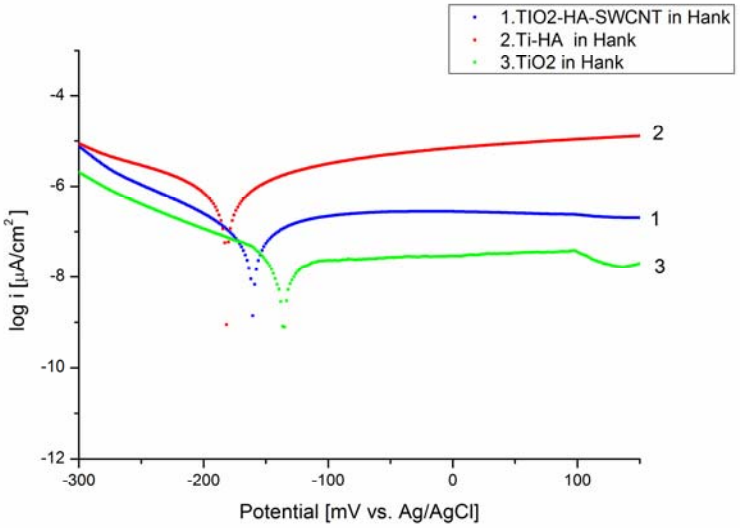

Fig.3. Polarization curves for TiO_2, TiO_2 –HA, TiO_2-HA-SWCNTs materials in Hank solution at 37°C

Table 5 presents the determined values of corrosion potential (E_{corr}), corrosion current densities (i_{corr}), anodic and cathodic Tafel slopes (b_a, b_c) and corrosion rate expressed in mm/year.

Table5

The electrochemical parameters obtained by extrapolation of Tafel curves for all three coated materials in Hank solution at 37°C

Working electrode	E_{corr}, mV/SCE	$i_{corr} \times 10^2$, $\mu A/cm^2$	b_a, mV/dec	b_c, mV/dec	Corrosion rate $\times 10^3$, mm/year
TiO_2	-132	0.18	129	-55	0.015
TIO_2-HA	-175	93.44	151	-140	7.936
TIO_2-HA-SWCNTs	-155	7.96	111	-79	0.676

It is known that a b_a value greater than b_c will be specific for a material that tends toward passivity, while a material with tendency to corrosion will have a b_a value smaller than b_c. In our case, if we compare b_a with b_c values for all samples, it can be observed that the occurring processes at the surface are under anodic control.

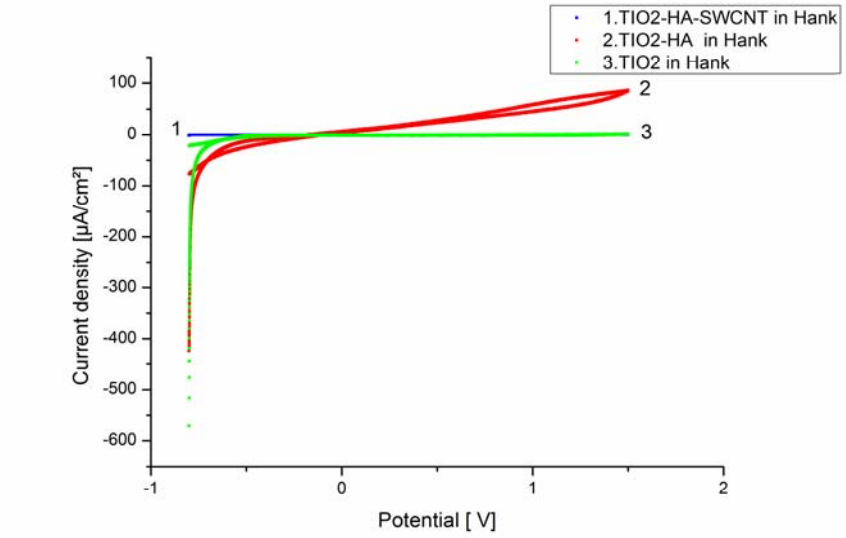

Fig.4. Cyclic voltammogram for TiO_2, TiO_2-HA, TiO_2-HA-SWCNTs material in Hank solution

From the obtained voltammogrames (Fig. 4) it can be seen that, except for TiO_2-HA, no breakdown phenomena were observed. For TiO_2-HA in Hank solution the breakdown potential was -90 mV and the repassivation potential was -172 mV.

The electrochemical impedance spectroscopy (EIS) measurements were performed at the open circuit potential and the spectra were acquired in a 100 kHz –50 mHz frequency range. The impedance spectra were presented both as Nyquist plots, where the imaginary component of the impedance is plotted as a function of the real component, and as Bode plots, where only the phase angle is plotted as a

function of the logarithm of the frequency. Fig. 5 presents the Nyquist spectra which indicate a decrease of corrosion resistance (if a decrease in semicircle diameter is considered) in the order: TiO_2, TiO_2-HA and TiO_2-HA-SWCNTs.

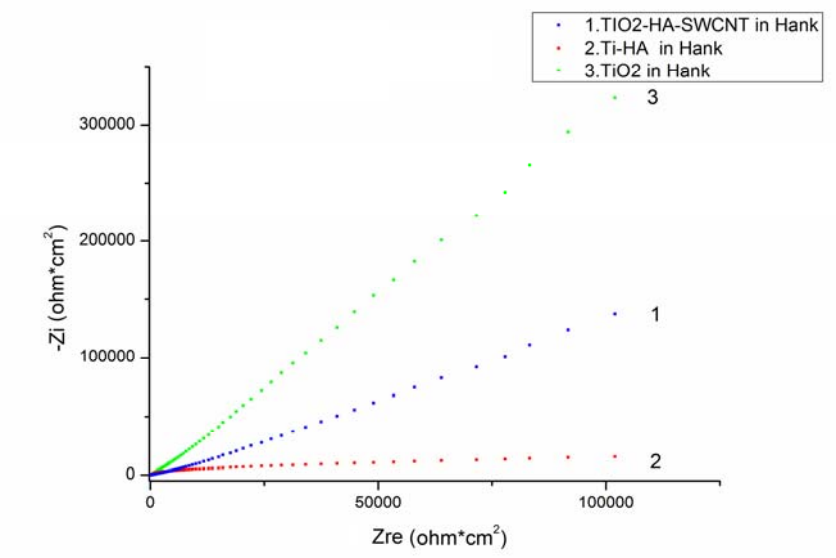

Fig.5. Nyquist diagram for TiO_2, TiO_2-HA, TiO_2–HA-SWCNTs in Hank solution at 37°C

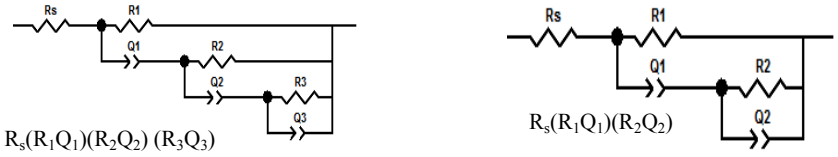

a) b)

Fig.6. Equivalent circuits used for a)TiO_2-HA, TiO_2-HA-SWCNTs and b) TiO_2 after immersion in Hank's solution; The software Zview was used.

Two equivalent circuit models, the first one $R_s(R_1Q_1)(R_2Q_2)$ and the second one $R_s(R_1Q_1)(R_2Q_2)(R_3Q_3)$, proposed also by other autors [19], were used for fitting the spectra for TiO_2, TiO_2-HA, TiO_2–HA-SWCNTs in Hank solution. Both are presented in Fig. 6 and correspond to a coating formed either as two superposed layers (barrier and porrous layers, Fig. 6a) or as a single layer (barrier layer, Fig. 6b). R_s is the solution resistance, R_1 - the resistance of barrier layer, Q_1 - the double layer capacitance of the barrier layer expressed as constant phase element, R_2 is the resistance of the porous layer, Q_2 is the double layer capacitance (constant phase element) of the porrous layer, R_3 is the polarization resistance of the apatite layer, Q_3 is the double layer capacitance (constant phase

element) of the apatite layer. The constant phase element introduced instead of pure capacitance is representing the non-ideal capacitive behavior of the films, and n_1, n_2 and n_3 are the exponents of the constant phase element, $0<n<1$, related to non-uniform current distribution due to surface roughness [20]. The obtained values of parameters are presented in Table 6.

Table 6

EIS spectra fitted values for TiO_2, TiO_2-HA, TiO_2 –HA-SWCNTs after immersion in Hank's solution

Circuit parameter	Coating		
	TiO_2	TiO_2-HA	TiO_2 –HA-SWCNTs
R_s, kΩcm^2	45	45	45
R_1, kΩcm^2	350.9	1250	1350
Q_1, μFcm^{-2}s^n	0.304	0.15	0.13
n_1	0.68	0.60	0.55
R_2, kΩcm^2	0.06	0.32	0.35
Q_2, μFcm^{-2} s^n	0.15	0.186	0.199
n_2	0.95	0.91	0.86
R_3, kΩcm^2	-	0.18	0.19
Q_3, μFcm^{-2} s^n	-	0.0158	0.804
n_3	-	0.93	0.96

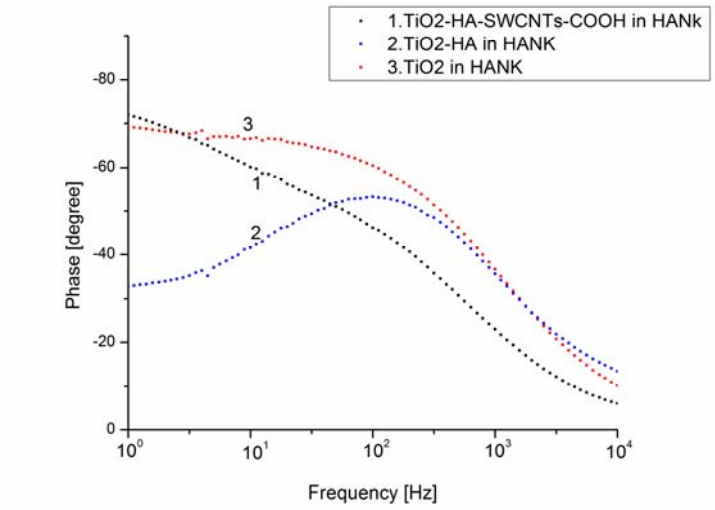

Fig.7. Bode diagram for TiO_2, TiO_2-HA, TiO_2–HA-SWCNTs in Hank solution

In Fig.7 the Bode diagrams show that the maximum phase angle for TiO_2 material is about -75^o for low frequency, suggesting a strong capacitive behavior; a slow decrease in the range of medium frequencies and a drastical decrease for higher frequencies are observed. For TiO_2–HA material the phase angle curve for

Hank solution has low values (around -32^o) for low frequencies, increases to a maximum phase angle (-60^o) for medium frequencies which suggest a diffusive behavior with weak capacitive trends and decreases again for high frequencies. The phase angle curve for TiO_2–HA-SWCNTs material is about -75^o (maximum value) for low frequncies, suggesting a strong capacitive behavior, then decreases continuously for medium and high frequencies.

4. Conclusions

The presence of phosphate, hydroxyl and carbonate groups within the new TiO_2-HA-SWCNTs coating was revealed in FT-IR analysis. The contact angles measurements using distilled water indicate for all investigated samples, TiO_2, TiO_2-HA and TiO_2-HA-SWCNTs a hydrophilic behavior. From the E_{OCP}-time curves is obtained a general tendency towards a stabile state in Hank solution at 37 °C for all three coatings. E_{OCP}-time quasi-linear curve remained in the positive domain of potential and has a slow ascendant trend for TiO_2-HA-SWCNTs, which can be explained by the fact that the new hybrid material tends to reach a nobler state compared with TiO_2 and TiO_2-HA.

The corrosion rate values for all three coatings immersed in Hank solution at 37 °C are in the perfect stable domain of corrosion resistance (on the corrosion scale) and no breakdown phenomena were observed from the obtained voltammograms, except for TiO_2-HA in Hank solution.

The impedance behavior shown in Nyquist diagrams is pretty similar for all samples, but the corrosion resistance (polarization resistance) in Hank solution at 37 °C decreases in the order: TiO_2, TiO_2-HA and TiO_2-HA-SWCNTs. From the Bode plots, we noticed that the maximum phase angle in Hank solution for TiO_2 and TiO_2–HA-SWCNTs is about -75^o, suggesting a strong capacitive behavior, then it decreases drastically for higher frequencies; this can indicate a dense barrier-type coating. In Hank solution TiO_2-HA coating shows a maximum phase angle about -60^o suggesting a diffusive behavior with weak capacitive trends; this may be connected to existence of a porous coating.

Based on our results we can recommend the new bionic coating TiO_2–HA-SWCNTs as suitable in bio applications, due to its strong hydrophilic character, good stability and corrosion resistance, as well as its structure of a dense barrier layer.

R E F E R E N C E S

[1]. *P. Tengvall and I. Lundstrom*,"Physico-chemical considerations of titanium as a biomaterial", Clin. Mater, **vol. 9**, 1992, pp. 115-34.

[2]. *M. Mindroiu, E. Cicek, F. Miculescu and I. Demetrescu,*"The influence of the rmaloxidationtreatment on the electrochemical stability of TiAlV and TiAlFe alloys and their potential application as biomaterials", Rev. Chim. (Bucharest), **vol. 58**, no. 9, 2007, pp. 898-903.

[3]. *D. Ionita, M. Grecu,C. Ungureanu and I. Demetrescu,*"Modifying the TiAlZr biomaterial surface with coating, for a better anticorrosive and antibacterial performance", J. Appl. Surface Sci., **vol. 21**, 2011, pp. 9164-9168.

[4].*C.C. Chen and S.J. Ding*, "Effect of heat treatment on characteristics of plasma sprayed hydroxyapatite coatings", Materials Trans., **vol. 47**, no. 3, 2006, pp. 935 -940.

[5] *S. Hiromoto and M. Tomozawa1*, "Corrosion behavior of magnesium with hydroxyapatite coatings formed by hydrothermal treatment", Materials Trans., **vol. 51**, no. 11, 2010, pp. 2080 -2087.

[6]. *X. Min, M. Fengcang, L. Ping, L. Wei, L. Xinkuan, C. Xiaohong, H. Daihua and G. Fang*, "Influences of pH value and deposition time on HA/TiO_2 coatings deposited by electrochemical method", Materials Trans., **vol. 55**, no. 6, 2014, pp. 937- 941.

[7]. *H. Tsutsumi1, M. Niinomi, M. Nakai, T. Gozawa, T. Akahori, K. Saito, R. Tuand and T. Goto*,"Fabrication of hydroxyapatite film on Ti-29Nb-13Ta-4.6Zr using a MOCVD technique", Materials Trans., **vol. 51**, no. 12, 2010, pp. 2277- 2283.

[8]. *M. Okido, K. Nishikawa, K. Kuroda, R. Ichino, Z. Zhao and O. Takai*,"Evaluation of the hydroxyapatite film coatting on titanium cathode by QCM" , MaterialsTrans., **vol. 51**, no. 12, 2010, pp. 2277- 2283.

[9]. *Y. Wang, J. Tao, L. Wang, P. He and T. Wang*, "HA coating on titanium with nanotubular anodized TiO_2 intermediate layer via electrochemical deposition", Trans. Nonferrous. Met. Soc. China, **vol. 18**, 2008, pp. 631-635.

[10]. *N.A.A. Mobarak and A.A.A. Swayih,* "Development of titanium surgery implants for improving osseointegration through formation of a titanium nanotube layer", Int. J. Electrochem. Sci., vol. **9**, 2014, pp. 32–45.

[11]. *S.Y. Madani , A. Tan, M. Dwek and A.M. Seifalian*, "Functionalization of single-walled carbon nanotubes and their binding to cancer cells", Int. J. Nanomedicine, **vol. 7**, 2012, pp. 905-914.

[12]. *J. Talla, D. Zhang, M. Kandadai, A. Avadhanula and S. Curran*, "A resonance Raman study of carboxyl induced defects in single-walled carbon nanotubes", Physica B, **vol. 405**, 2010, pp. 4570–4573.

[13]. *K. Mallick and A.M. Strydom*, "Biophilic carbon nanotubes", Colloids Surf. B: Biointerfaces , **vol. 105**, 2013, pp. 310– 318.

[14]. *B.D. Hahn, J.M. Lee, D.S. Park, J.J. Choi, J. Ryu, W.H. Yoon, B.K. Lee, D.S. Shin and H.E. Kim*, "Mechanical and in vitro biological performances of hydroxyapatite-carbon nanotube composite coatings deposited on Ti by aerosol deposition", Acta Biomater, **vol. 5**, 2009, pp. 3205-3214.

[15]. *M. Prodana, M. Duta, D. Ionita, D. Bojin, M.S. Stan, A. Dinischiotu and I. Demetrescu*, "A new complex ceramic coating with carbon nanotubes, hydroxyapatite and TiO_2 nanotubes on Ti surface for biomedical applications", Ceramics Int.,**vol. 41, 5** 2015, pp. 6318-6325.

[16]. *M.N. Tchoul, W.T. Ford, G. Lolli, D.E. Resasco and S. Arepalli*, "Effect of mild nitric acid oxidation on dispersability, size, and structure of single-walled carbon nanotubes", Chem. Mater., **vol. 19**, 2007, pp. 5765-5772.

[17]. *C.C. Ciobotaru, C.M. Damian and H. Iovu*, "Single-wall carbon nanotubes purification and oxidation", U.P.B. Sci. Bull., Series B, vo**l. 75**, no. 2, 2013, pp. 55 – 66.

[18]. *I. Man, C. Pirvu and I . Demetrescu,* "Enhancing titanium stability in Fusayama saliva using electrochemical elaboration of TiO_2 nanotubes", Rev. Chim. (Bucharest), **vol. 59**, no. 6, 2008, pp. 615-617.

[19]. *K. Indira, U. Kamachi Mudali and N. Rajendran,* "Corrosion behavior of electrochemically assembled nanoporous titania for biomedical applications", Ceramics Int.,**vol. 39, 2013,** pp. 959–967.

[20]. *J. Liu, J. Yi, S. Li, M. Yu, G. Wu and L. Wu,* "Effect of electrolyte concentration onmorphology, microstructure and electrochemical impedance of anodic oxide film on titanium alloy Ti–10V–2Fe–3Al", J. Appl. Electrochem., **vol. 40, 2013,** pp. 1545–1553.